

Article

# Spatial and Seasonal Variation of O and H Isotopes in the Jiulong River, Southeast China

Kunhua Yang , Guilin Han \* , Man Liu, Xiaoqiang Li , Jinke Liu and Qian Zhang

School of Scientific Research, China University of Geosciences, Beijing 100083, China; kunhuayang@cugb.edu.cn (K.Y.); lman@cugb.edu.cn (M.L.); xiaoqli@cugb.edu.cn (X.L.); liujinke@cugb.edu.cn (J.L.); zhangqian9@cugb.edu.cn (Q.Z.)

\* Correspondence: hanguilin@cugb.edu.cn; Tel.: +86-010-8232-3536

Received: 14 October 2018; Accepted: 14 November 2018; Published: 17 November 2018



**Abstract:** The stable isotope technique of oxygen and hydrogen ( $\delta^{18}\text{O}$  and  $\delta^2\text{H}$ ) and deuterium excess ( $d$ -excess) was used to investigate distribution characteristics in June 2017 and January 2018 in the Jiulong River, southeast China. The results revealed that (1) seasonal isotopic composition was mainly controlled by precipitation. It enriched lighter water isotopes in winter more than in summer because of the aggravating effect of low temperature and great rainfall. (2) Spatial distribution of the North, West, and South River showed increasing enrichment of heavy isotopes in that order. In the high-flow season, the continuous high-flow made  $\delta^{18}\text{O}$  and  $\delta^2\text{H}$  homogeneous, despite increasing weak evaporation along water-flow paths in the West and South River. In the low-flow season, there was a decreasing trend in the middle and lower reaches of the North and West main stream and an increasing trend in the South River. (3) O and H isotopic geochemistry exhibited natural and anthropogenic influence in hydrological process, such as heavy rainfall and cascade reservoirs. The results showed that O and H isotopes are indeed useful tracers of the water cycle.

**Keywords:**  $\delta^{18}\text{O}$ ;  $\delta^2\text{H}$ ; deuterium excess; spatial and seasonal variation; reservoirs; southeast China

## 1. Introduction

The stable O and H isotope technique has been demonstrated for application to hydrological models from local and regional to meso and global scales [1–4]. Long-term and large-scale isotope data indicated that the spatiotemporal pattern of precipitation was directly reflected in the water of most rivers [5]. The stable isotope composition in river water may be closely associated with precipitation events in some regions, which means that local climatic signals (e.g., humidity, temperature, and precipitation amount) can be recorded in the hydro-archive, such as river water, groundwater, or lacustrine sediment samples [6–12].

On a local scale, the change of hydrological processes may influence biogeochemical cycles for the ecosystem, especially in the process of precipitation recharging river water [13–18]. Determining how hydrological processes vary spatially and temporally can enhance our understanding and management of land use and climate change that impacts on rivers [19]. To solve water resources and relative environmental issues, many scientists have researched water cycle evolution using the stable water isotopes in river basins [6,7].

Surface water isoscapes had been developed and analyzed at large scale more frequently [20]. It was found that the average isotopic composition of river water reflected the average rainwater amount on a regional as well as global scale [2,21–23]. In large and medium scale catchments, the river water isotopes were also associated with water–rock interaction [24,25]. The catchment-constrained and global model demonstrated the isotopic correlation between average rainfall and river discharge and had predicted that the isotope composition of river water is controlled by the isotope composition

of precipitation [2,26]. H and O isotopes of river water across the USA reflected the regional meteoric patterns. Meanwhile, they were not significantly altered by evaporation, homogenization, or mixing with groundwater [6]. In a small basin with a complex climate system, such as the Olt River basin, water in tributaries enriched with  $^{18}\text{O}$  and  $^2\text{H}$  and showing bigger seasonal variation was considered as a consequence of lower flow and precipitation recharge source, however, the main stream water was depleted of  $^{18}\text{O}$  and  $^2\text{H}$  and had smaller variation, which can be explained by dams and discharge of groundwater which had almost constant isotopic composition [7,27]. Together, variation in the stable isotope composition and deuterium excess of river water may be able to identify source water dynamics associated with the synoptic weather systems, geographical variation of precipitation, and other factors [19,28].

It was demonstrated that the oxygen and hydrogen isotope composition of precipitation events and deuterium excess responded sensitively to complex moisture sources in some regions which have two or more types of synoptic weather systems [9,28,29]. In short, the pattern of stable isotope composition of precipitation was linked to the local climate. On the other hand, the isotopic composition of river water was likely more representative of the water used by plants and organisms within the watershed [22], which was closely associated with the hydrological and biogeochemical cycle of the ecosystem. Therefore, more research of spatial and seasonal variation in O and H isotopes in river water are significantly important.

However, the study of the isotopic composition of surface river water at a medium-sized coastal watershed was relatively low, especially at a low-latitude-oceanic-monsoon coastal watershed. The Jiulong River is the second largest river in Fujian province, southeast China, and it plays an important role in regulating, storing, and supplying water for the local socio-economy. In this study, we conducted research on the Jiulong River and present the results of isotopic investigations in June 2017 and January 2018. This paper reports the spatial distribution and seasonal variation of O and H isotopes in the Jiulong River, including three tributaries and the estuary, in order to investigate how multiple factors affect the isotopic variation of river water. The findings are likely to provide a better understanding of processes controlling the stable isotopes of river water in coastal watersheds of southeast China.

## 2. Materials and Methods

### 2.1. Background of the Study Area

Jiulong River is located in Fujian Province, southeast China ( $24^{\circ}18' \sim 25^{\circ}88' \text{ N}$ ,  $116^{\circ}78' \sim 118^{\circ}03' \text{ E}$ ), which has a  $14,087 \text{ km}^2$  drainage basin (Figure 1). The study area is dominated by subtropical oceanic monsoon conditions. There was about 75% discharge and rainfall annually from April to September in the North River (Pu-nan station) and the West River (Zhengdian station) [30,31]. The Jiulong River catchment has an important impact on socio-economic development and the natural environment of southwestern Fujian Province, partly because of many cascade reservoirs and hydropower stations along the North and West River (Figure 1).

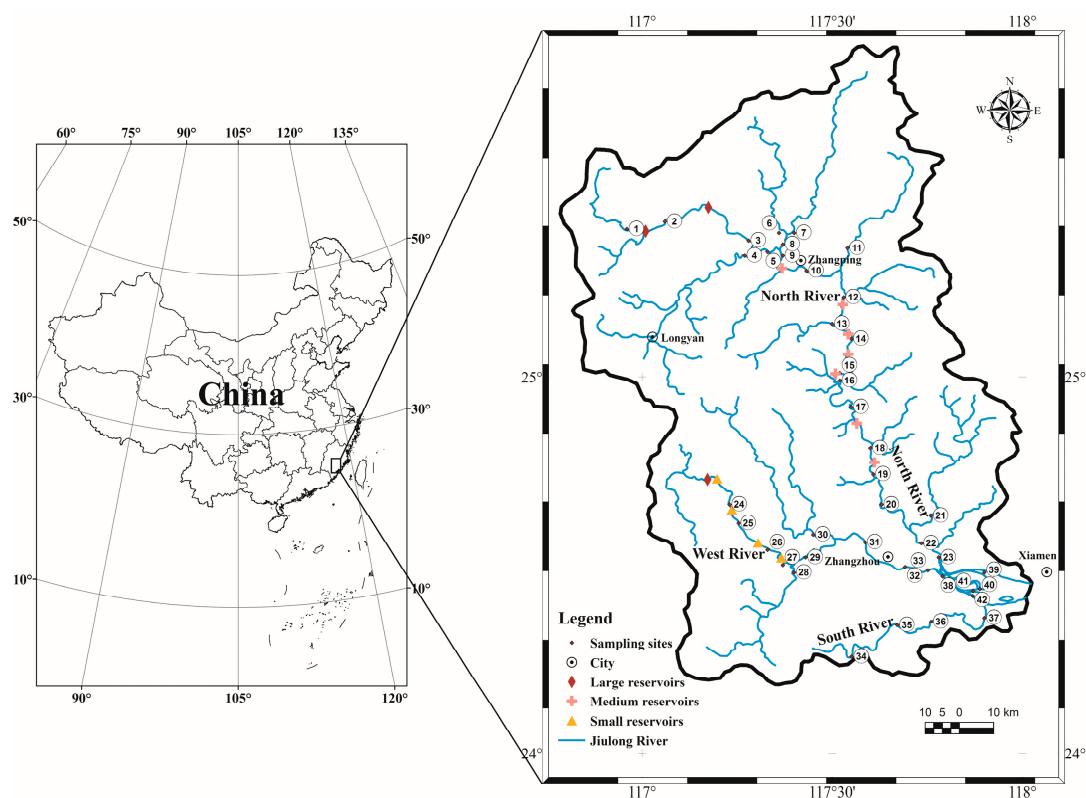


**Figure 1.** Drainage map of the Jiulong River and the sampling sites.

## 2.2. Water Collection and Analytical Methods

Forty-two surface river water sampling sites were set along Jiulong River, its main tributaries, and estuary in June 2017 and January 2018, the high-flow season and low-flow season, respectively (Figure 1). From headstream to estuary, twenty-three sample sites are located in the North River, ten in the West River, four in the South River, and five in the estuary, each as inferred from hydrological condition, lithology, and land use. Water samples were filtered using a cellulose acetate membrane (0.22  $\mu\text{m}$ ) in situ, and stored in 2 mL pre-cleaning glass bottles. The bottle must be full with sample water and sealed. Electrical conductivity (EC) and temperature measurements of bulk river water were taken using a YSI multi-parameter meter. The geographical coordinates and altitudes of sampling sites were determined by GPS.

The water samples were analyzed for  $\delta^{18}\text{O}$  and  $\delta^2\text{H}$  with Triple-Liquid Water Analyzers (TIWA-45-EP) (LGR, San Jose, CA, USA) by laser spectroscopy techniques at the Institute of Geographic Sciences and Natural Resources Research, Chinese Academy of Sciences, China. All the isotope data were reported in per mill (‰) relative to Vienna Standard Mean Ocean Water (V-SMOW), and the measurement precision was  $\pm 0.1\text{‰}$  ( $1\sigma$ ) for  $\delta^{18}\text{O}$  and  $\pm 0.5\text{‰}$  ( $1\sigma$ ) for  $\delta^2\text{H}$ . The relative deviation of the isotopic ratio of the sample and standard was calculated as:

$$\delta^{18}\text{O} (\text{‰}) = \left[ \frac{(^{18}\text{O}/^{16}\text{O})_{\text{sample}}}{(^{18}\text{O}/^{16}\text{O})_{\text{standard}}} - 1 \right] \times 10^3 \quad (1)$$

$$\delta^2\text{H} (\text{‰}) = \left[ \frac{(^2\text{H}/^1\text{H})_{\text{sample}}}{(^2\text{H}/^1\text{H})_{\text{standard}}} - 1 \right] \times 10^3 \quad (2)$$

## 2.3. Indication of Other Data

We analyzed the spatial and temporal distribution of deuterium excess, which is defined as  $d\text{-excess} = \delta^2\text{H} - 8\delta^{18}\text{O}$  [32]. In addition, we collected stable hydrogen and oxygen isotope data of precipitation in the Fuzhou station, which is close to our study area, from The Global Network of Isotope in Precipitation (GNIP) [33] that was initiated in 1958 by International Atomic Energy Agency

(IAEA) and World Meteorological Organization (WMO). All data for GNIP can be downloaded in CSV or Microsoft Excel flat files, cost-free to registered users, in IAEA website [34].

### 3. Results

On the Jiulong River catchment, the  $\delta^{18}\text{O}$  values of river water ranged from  $-8.18\text{‰}$  to  $-6.54\text{‰}$  in June 2017 and from  $-9.37\text{‰}$  to  $-5.62\text{‰}$  in January 2018, whereas  $\delta^2\text{H}$  values ranged from  $-52.9\text{‰}$  to  $-42.8\text{‰}$  and from  $-60.8\text{‰}$  to  $-38.1\text{‰}$ , respectively (Table 1). Mean values of  $\delta^{18}\text{O}$  and  $\delta^2\text{H}$  were calculated as  $-7.29\text{‰}$  and  $-47.1\text{‰}$  in summer and  $-7.84\text{‰}$  and  $-52.1\text{‰}$  in winter. From north to south (North River, West River, South River, estuary), the mean values of  $\delta^{18}\text{O}$  were  $-47.8\text{‰}$ ,  $-46.9\text{‰}$ ,  $-43.7\text{‰}$ , and  $-46.9\text{‰}$  in the high-flow season and were  $-55.1\text{‰}$ ,  $-50.0\text{‰}$ ,  $-42.1\text{‰}$ , and  $-50.0\text{‰}$  in the low-flow season, while the mean values of  $\delta^2\text{H}$  were  $-7.42\text{‰}$ ,  $-7.28\text{‰}$ ,  $-6.70\text{‰}$ , and  $-7.22\text{‰}$  in the high-flow season and that were  $-8.32\text{‰}$ ,  $-7.64\text{‰}$ ,  $-6.10\text{‰}$ , and  $7.41\text{‰}$  in the low-flow season. In a word,  $^{18}\text{O}$  and  $^2\text{H}$  were generally depleted with increasing latitude.

**Table 1.** Locations and isotope composition of the water samples in this study.

Sampling Site	Latitude (N)	Longitude (E)	Altitude (m)	High-Flow Season			Low-Flow Season			
				$\delta^2\text{H}$ (‰)	$\delta^{18}\text{O}$ (‰)	<i>d</i> -Excess (‰)	$\delta^2\text{H}$ (‰)	$\delta^{18}\text{O}$ (‰)	<i>d</i> -Excess (‰)	
North River	1	116.96	25.39	384	-52.9	-8.18	12.6	-57.2	-8.65	12.0
	2	117.06	25.41	282	-46.8	-7.50	13.2	-51.4	-7.94	12.1
	3	117.28	25.36	206	-48.1	-7.62	12.9	-51.8	-7.90	11.4
	4	117.27	25.32	197	-46.3	-7.36	12.6	-48.7	-7.09	8.0
	5	117.33	25.33	173	-47.6	-7.37	11.4	-51.4	-7.72	10.4
	6	117.36	25.38	182	-48.7	-7.56	11.8	-60.8	-9.37	14.2
	7	117.40	25.38	174	-45.2	-7.11	11.6	-59.0	-9.15	14.2
	8	117.37	25.35	162	-45.4	-6.99	10.5	-57.3	-8.67	12.1
	9	117.37	25.32	172	-47.2	-7.35	11.6	-51.1	-7.87	11.9
	10	117.44	25.28	159	-46.8	-7.25	11.1	-52.9	-8.00	11.2
	11	117.54	25.34	177	-47.0	-7.26	11.1	-51.6	-7.73	10.2
	12	117.53	25.21	143	-47.8	-7.47	12.0	-54.2	-8.21	11.5
	13	117.50	25.14	153	-51.6	-7.91	11.7	-55.8	-8.44	11.7
	14	117.55	25.10	109	-47.7	-7.37	11.2	-57.5	-8.76	12.5
	15	117.52	25.01	89	-47.7	-7.50	12.3	-57.3	-8.71	12.4
	16	117.52	24.99	83	-50.2	-7.66	11.1	-49.6	-7.62	11.3
	17	117.55	24.92	35	-48.0	-7.47	11.8	-59.4	-8.90	11.8
	18	117.60	24.81	27	-48.2	-7.51	11.9	-57.9	-8.58	10.7
	19	117.60	24.74	16	-48.2	-7.48	11.6	-59.1	-8.84	11.5
	20	117.63	24.66	8	-47.2	-7.09	9.5	-59.1	-8.81	11.4
	21	117.76	24.63	13	-45.4	-6.78	8.8	-45.8	-6.66	7.5
	22	117.74	24.56	7	-47.9	-7.32	10.7	-59.6	-8.84	11.2
	23	117.78	24.52	29	-47.9	-7.54	12.4	-59.1	-8.96	12.6
West River	24	117.23	24.66	136	-49.3	-7.62	11.7	-48.6	-7.41	10.7
	25	117.25	24.61	78	-48.5	-7.50	11.5	-50.3	-7.53	9.9
	26	117.33	24.54	37	-48.1	-7.49	11.8	-48.2	-7.46	11.5
	27	117.37	24.50	23	-47.3	-7.40	11.9	-47.5	-7.09	9.2
	28	117.40	24.48	24	-43.7	-6.89	11.4	-48.6	-7.40	10.6
	29	117.43	24.52	20	-46.2	-7.24	11.7	-48.2	-7.60	12.6
	30	117.45	24.58	27	-47.4	-7.32	11.2	-51.2	-7.86	11.7
	31	117.59	24.56	16	-46.2	-7.13	10.9	-52.9	-8.16	12.4
	32	117.69	24.50	1	-46.2	-7.16	11.0	-51.5	-7.67	9.8
	33	117.75	24.49	1	-46.4	-7.09	10.3	-53.4	-8.21	12.3
	South River	34	117.55	24.26	70	-45.4	-6.98	10.5	-43.3	-6.52
35		117.67	24.34	16	-43.6	-6.69	9.8	-42.6	-6.15	6.6
36		117.76	24.35	7	-43.2	-6.58	9.5	-44.1	-6.09	4.6
37		117.90	24.36	-1	-42.8	-6.54	9.5	-38.1	-5.62	6.8
Estuary	38	117.79	24.47	7	-46.9	-7.23	10.9	-54.7	-8.27	11.5
	39	117.90	24.48	-2	-47.4	-7.41	11.9	-56.0	-8.61	12.9
	40	117.89	24.44	0	-46.0	-7.08	10.7	-45.6	-6.55	6.7
	41	117.87	24.43	0	-47.1	-7.11	9.8	-46.8	-6.61	6.0
	42	117.86	24.42	5	-47.0	-7.28	11.2	-46.9	-7.01	9.2

The relation between  $\delta^{18}\text{O}$  and  $\delta^2\text{H}$  values for all river water samples with the global meteoric water line (GMWL  $\delta^2\text{H} = 8\delta^{18}\text{O} + 10$  [35]) and Local Meteoric Water Line (LMWL1 [33] and LMWL2 [36]) was presented in Figure 2. LMWL1 was obtained from the Global Network of Isotope in Precipitation [33] and we selected the database of the closest station Fuzhou to form the LMWL1, which, with a slope of 8.19 and an intercept of 11.73, was not statistically different from the GMWL. LMWL2 of Zhangzhou was  $\delta^2\text{H} = 8.02\delta^{18}\text{O} + 9.11$  which was quoted from the reference [36]. Most of the Jiulong River water laid to the left of or on the GMWL (Figure 2). In June 2017, river water fell on the left of GMWL and LMWL. Differently, the plots of river water in January 2018 fell on two sides of GMWL and LMWL. The  $\delta^{18}\text{O}$  value of  $-7\text{‰}$  divided the water samples in January 2018 into two parts, of which the heavier part had obviously higher EC values (Figure 3). The river water sampled in November 1985 and August 1986 plotted below and to the right of the GMWL and were near the Jiulong River line in this study, whereas the spring water sampled in August 1986 were near the GMWL and plotted behind and far from the GMWL for which sampled in November 1985 [36].

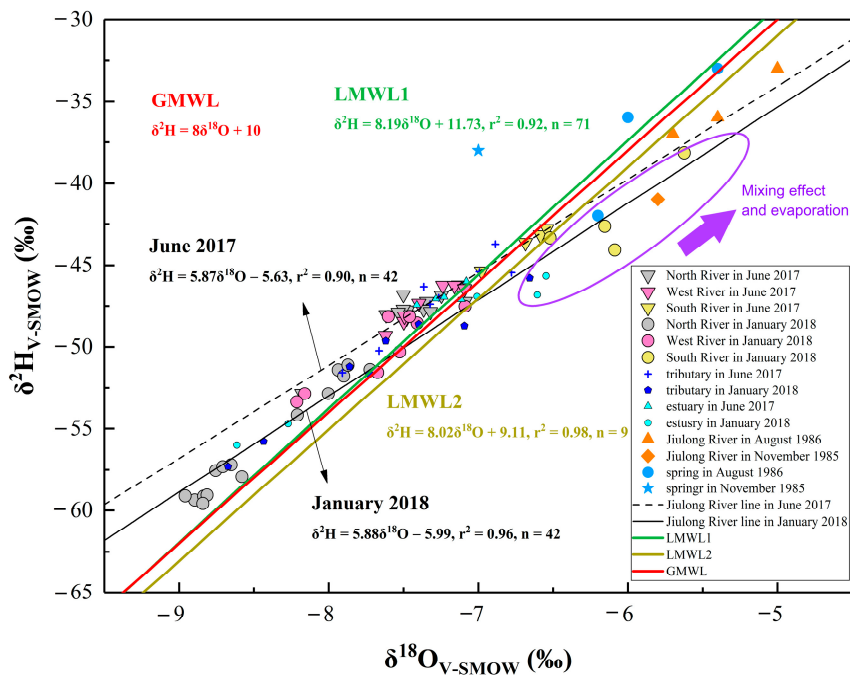


**Figure 2.** Correlations between  $\delta^{18}\text{O}$  and  $\delta^2\text{H}$  in the Jiulong River water. The  $\delta^{18}\text{O}$  and  $\delta^2\text{H}$  of river water and spring which were sampled in August 1986 and November 1985 were quoted from reference [36]. GMWL: Global Meteoric Water Line [35]. LMWL1: Meteoric Water Line of Fuzhou [33]. LMWL2: Meteoric Water Line of Zhangzhou [36].

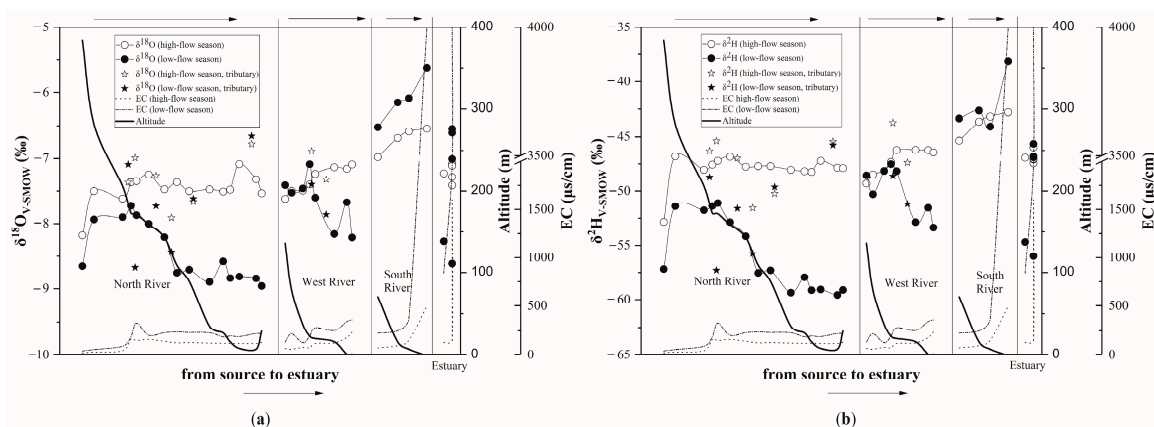


**Figure 3.** O (a) and H (b) isotope composition of all samples in different seasons.

Spatial distribution of  $\delta^{18}\text{O}$  and  $\delta^2\text{H}$  of the Jiulong River water together with altitude and electrical conductivity in two seasons was presented (Figure 3). In general, both oxygen and hydrogen isotopes showed different composition patterns in the different seasons for each river. From source water toward the estuary, the  $\delta^{18}\text{O}$  and  $\delta^2\text{H}$  in June 2017 for three tributaries exhibited no significant difference except for the heavier samples in the lower reach of South River, which had higher EC values than the upper-middle reaches caused by the evaporation and the mixing of river water and seawater. However, this mixture did not make the plots in summer deviate from the Jiulong River line or lie underneath GMWL (Figure 2). In January 2018, there was clear difference between each riverine isotope composition. From Site No. 10 to downstream in the North River and along the West River, there was a generally decreasing trend of  $\delta^{18}\text{O}$  and  $\delta^2\text{H}$  values in January 2018, however, the contrary trend happened in the South River likely because of the increasing mixing with seawater.

The seasonal variation of O and H isotopic composition is illustrated in Figures 3 and 4, which shows that the range of  $\delta^{18}\text{O}$  and  $\delta^2\text{H}$  in June 2017 was smaller than that in January 2018. During the high-flow season (June 2017), box diagrams for  $\delta^{18}\text{O}$  and  $\delta^2\text{H}$  showed that most of the data of Jiulong River water displayed a narrow range, while it was wider in the low-flow season (January) (Figure 4). This suggested that O and H isotopic distribution of the Jiulong River had small difference and was heavier overall in the high-flow season, whereas it was more dispersive and lighter in the low-flow season. The main stream of North River and West River had much variation in isotope composition for two seasons in the middle and lower reaches, on the contrary, the tributaries in the North River had a larger difference in the upper and middle reaches. Overall, water isotope composition, ordered from light to heavy, was as follows: North, West, and South River.

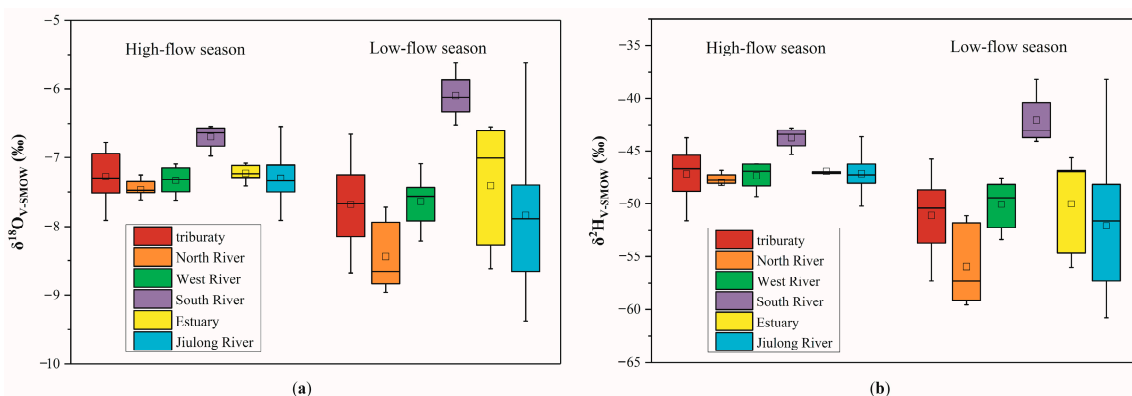


**Figure 4.** Box diagrams for  $\delta^{18}\text{O}$  (a) and  $\delta^2\text{H}$  (b) in the high-flow season and low-flow season of the main stream and its tributaries in the Jiulong River.

## 4. Discussion

### 4.1. Deuterium Excess (*d*-Excess)

The oxygen and hydrogen isotope composition and *d*-excess values suggested that the Jiulong River water was mainly derived from rainfall and lacked significant evaporation. However, several water samples in the South River and estuary in winter fell to the right of the GMWL and LMWL (yellow and blue circles in the purple ellipse in Figure 2) and had low *d*-excess values and high EC values (Figure 5), and we interpreted this as the consequence of evaporation and mixing with seawater (Figure 3).

The *d*-excess of rainwater cannot be influenced by precipitation amount, trajectory of air mass, nor latitude during precipitation [37]. However, evaporative vapor from the water's surface and the effect of secondary evaporation can make the *d*-excess of precipitation change as well as the surface water [3,38,39]. At the global scale, average *d*-excess of precipitation is 10‰, in fact, which can vary. According to the reference [40], the rate of evaporative vapor was 2.2% on average and the effect of secondary evaporation was not obvious in the summer in our study area. We assumed they were less

and weaker in winter since there was lower mean temperature in winter and a significantly larger amount rainfall in January 2018 than in January 2000–2017 (Table A1). Therefore, it is suggested that the  $d$ -excess value of meteoric water should be close to 10‰ in the Jiulong River catchment and is effectively 11.73‰ and 9.11‰ for the intercept of LMWL1 and LMWL2, respectively (Figure 2).

The  $d$ -excess was validly demonstrated in tracing the water cycle at a catchment scale [11,37,41]. In this study, the  $d$ -excess values of all the river water samples mostly ranged from 6‰ to 15‰ (Figure 5). In June 2017, most  $d$ -excess data generally decreased downstream and ranged from 8.8‰ to 13.2‰, which is close to the annual mean  $d$ -excess values of rainwater in Xiamen, i.e.,  $10.95 \pm 1.77$ ‰ [42]. The main reason was decreasing mean temperature with the distance-from-coast in the Jiulong River catchment, which can weaken the evaporation and make  $^{16}\text{O}$  and  $^1\text{H}$  enriched in river water with decreased  $d$ -excess value [39]. In January 2018, all of the  $d$ -excess values were more fluctuant and seemingly irregular, and six samples in the South River and estuary had very low  $d$ -excess values, likely because of mixing with seawater (Figure 5). In general, the  $d$ -excess values in the low-flow season did not reflect the continuous evaporation effect in the runoff direction, and the fluctuations may reflect the mixing effect of discharging river water with different sources. The  $d$ -excess values of fresh water didn't show significant seasonal differences in this study area, which was different from previous studies [8,43] showing that  $d$ -excess values were higher in summer. We considered this a consequence of the same water vapor source in summer and winter [44,45] and the large rainfall amount in January 2018.

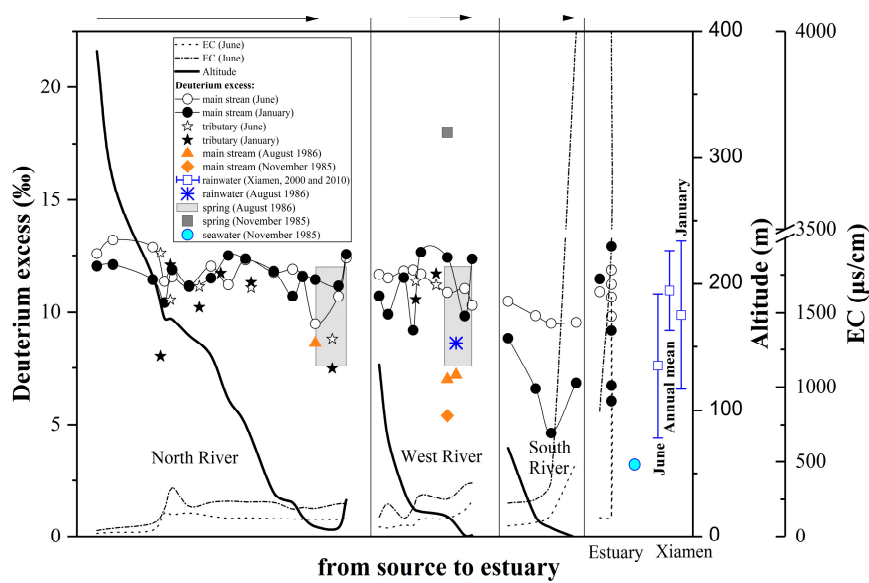


**Figure 5.** Spatial and seasonal variation of deuterium excess of river water, rainwater and spring in the Jiulong River basin. The  $d$ -excess values of rainwater were quoted from references [36,42,44]. The  $d$ -excess values of spring were quoted from references [36]. The  $d$ -excess value of seawater was quoted from reference [36].

In Figure 5, according to the  $d$ -excess values of the two end-members (rainwater and spring), the range of deuterium excess implied that in both summer and in winter, the source of river water can include rainwater and groundwater and possibly anthropogenic input. In other words, it was difficult to distinguish their contributions, although the groundwater was supplied by rainwater. In conclusion, the spatial characteristics of the  $d$ -excess values in the Jiulong River were influenced by weak evaporative isotopic effects in June 2017, however, in January 2018, this evaporation effect was not clear or covered by different water sources.

4.2. Temporal and Spatial Variability of River Water Isotope Composition

In Figures 3 and 6, the  $\delta^{18}\text{O}$  and  $\delta^2\text{H}$  values in the low-flow season were lower than that in the high-flow season in the North and West River, which were opposite to the South River, the Mulanxi River, and the Minjiang River [46,47]. This was probably because the Mulanxi river water was mainly recharged by groundwater and the Minjiang river water experienced more evaporation in the dry season, however, the factors impacting the isotope composition were different in the North and West River due to the large rainfall amount and low evaporation according to our explanation in Section 4.1. On the other hand, typhoon “Saola” and “Haikui” in August 2012 and “Matmo” in July 2014 caused rainfall enriching of lighter isotopes, and warm, moist air masses during the summer monsoon had already been depleted of heavy isotopes due to progressive fractionation by travelling a long distance over the sea, which may have caused a large amount of rainfall to enrich the Minjiang River and the Mulanxi River with light isotopes [42,47,48]. During the sampling period, there was no typhoon directly influencing the Jiulong River catchment.

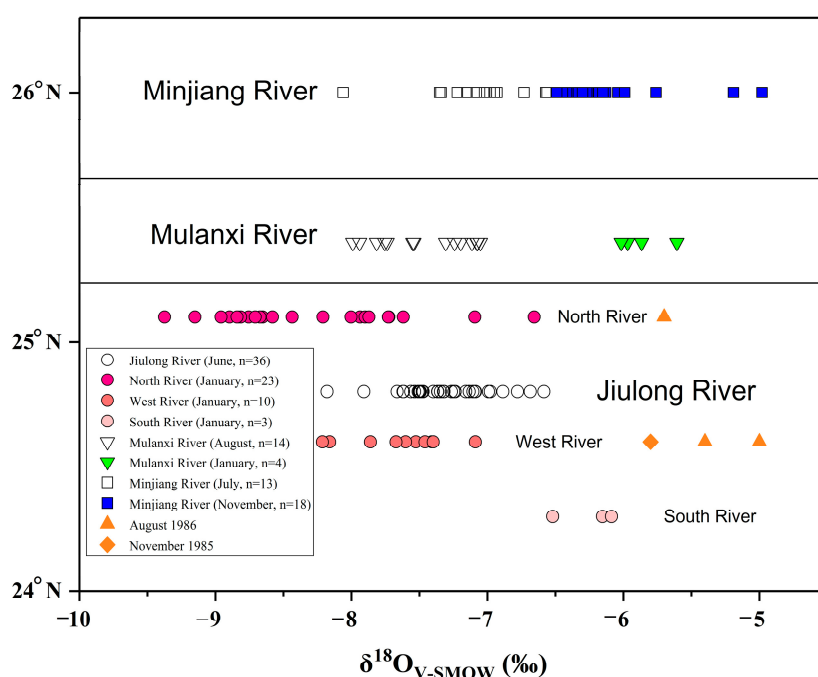


Figure 6. Fresh water oxygen isotope composition of the Jiulong River, the Mulanxi River [47], and the Minjing River [46] in southeast China.

In the upper reaches of the North River (i.e., before Zhangping city), the water isotope composition was about 0.5‰ and 10‰ higher in summer than in winter for  $\delta^{18}\text{O}$  and  $\delta^2\text{H}$ , respectively. The water isotopes became gradually lighter in the middle and lower reaches of the North River in winter, however, it was generally relatively stable in summer. For the West River, the trend was similar to the North River along the middle and lower reaches, and almost the same between the two seasonal samples in the upper reaches. For the South River, O and H isotopes were heavier in winter than in summer, and  $\delta^{18}\text{O}$  and  $\delta^2\text{H}$  values were increasing away from the water source in both seasons. To determine the factors that impact the spatial and seasonal variation in the Jiulong basin, firstly, we should understand what caused the differences among the three rivers. According to the “amount effect”, the average  $\delta^{18}\text{O}$  and  $\delta^2\text{H}$  values in the three tributaries were related to regional rainfall amount. We selected the monthly rainfall in Longyan, Zhangzhou, and Xiamen [31] to represent that

in the North, West, and South River. The relationship between  $\delta^{18}\text{O}$  and rainfall amount in June 2017 (Equation (3)) and January 2018 (Equation (4)) was:

$$\delta^{18}\text{O} (\text{‰}) = -0.0033A - 5.8297 \quad (r^2 = 0.80) \quad (3)$$

$$\delta^{18}\text{O} (\text{‰}) = -0.0267A - 2.9140 \quad (r^2 = 0.72) \quad (4)$$

where A is the monthly rainfall amount ( $\text{mm month}^{-1}$ ). In addition, the monthly rainfall amount was increasing in Longyan, Zhangzhou, and Xiamen both in summer and winter. Therefore, the  $\delta^{18}\text{O}$  values were decreased due to the increasing rainfall in the region, which was in accordance with the “amount effect”.

Seasonal variation in the H and O isotopic composition of river water was closely coupled to precipitation and relatively more stable [22]. Therefore, there was a strong isotopic correlation between average rainfall and river discharge in most regions. In other words, we can predict the isotope composition of rainwater and river water from each other. According to the literature [44,45], the “seasonal effect” that influenced the H and O isotopes of rainfall in Xiamen (i.e., the lower reach area) was very weak, such that it was covered by the “amount effect”, which meant that the  $\delta^{18}\text{O}$  and  $\delta^2\text{H}$  were lighter in summer because of the larger rainfall amount than in winter. Due to the river water responding quickly to precipitation in the small basin [49], in the South River (relatively close to Xiamen and coast), the water isotope composition was lighter in summer than in winter. Except for the “amount effect”, the precipitation isotopic variation was controlled by the temperature, latitude, altitude effects, and source of vapor [8,32]. From the coast to inland areas, the “amount effect” was generally weakened and the “seasonal effect” was relatively enhanced. In addition, in January 2018, the larger amount rainfall than previous years caused strong “amount effect”. Hence, the North River water was enriched with  $^{16}\text{O}$  and  $^1\text{H}$  in winter. Furthermore, the “altitude effect” was shown in Site 1 where water samples had light water isotopes.

#### 4.3. Impacts of Cascade Reservoirs on the Water Cycle

In the North River, there are two large reservoirs (storage capacity  $>0.1 \text{ km}^3$ ) and one medium reservoir (storage capacity:  $0.01 \text{ km}^3$ – $0.1 \text{ km}^3$ ) in the upper reach and six medium reservoirs in the mid-lower reaches, however, there is only one large reservoir and four small reservoirs (storage capacity  $<0.01 \text{ km}^3$ ) in the upper West River (Figure 1). According to Deng [37], the large-scale construction of impounding river had increased the residence time and enhanced the mixing of reservoir water derived from upstream. Consequently, it eventually resulted in the homogenization of reservoir water. Hence, in the reach of Sites 2–9,  $\delta^{18}\text{O}$  and  $\delta^2\text{H}$  values of river water were homogeneous both in summer and winter (Figures 3 and 7). Medium and small reservoirs should sustain releasing surplus water when the flow was too high and the reservoir water was close to storage capacity. Hence, a large amount rainfall and opening flood discharge during the summer caused continuous high flow in the North and West River which had homogeneous water isotopes. However, the reservoirs tended to store more water [50], especially in winter or low-flow season, causing decreased discharge downstream in the mid-lower reaches. In Figure 5, the *d*-excess in the mid-lower reaches of the North River suggested that the water isotopes were mainly controlled by rainfall in winter, although it was possibly affected by other factors, such as injection of groundwater and anthropogenic processes. Therefore, the river water that was divided into many sections by medium reservoirs had stored the information of mixing with rainwater, which was shown in the H isotope composition (Figure 7). Instead, the water isotopes in the mid-lower reaches were generally lighter downstream because of the increasing mixing proportion with rain water. However, in the low-flow season, it was more complex in the West River, which was explicable by the different water source, water storage, and evaporation [46].

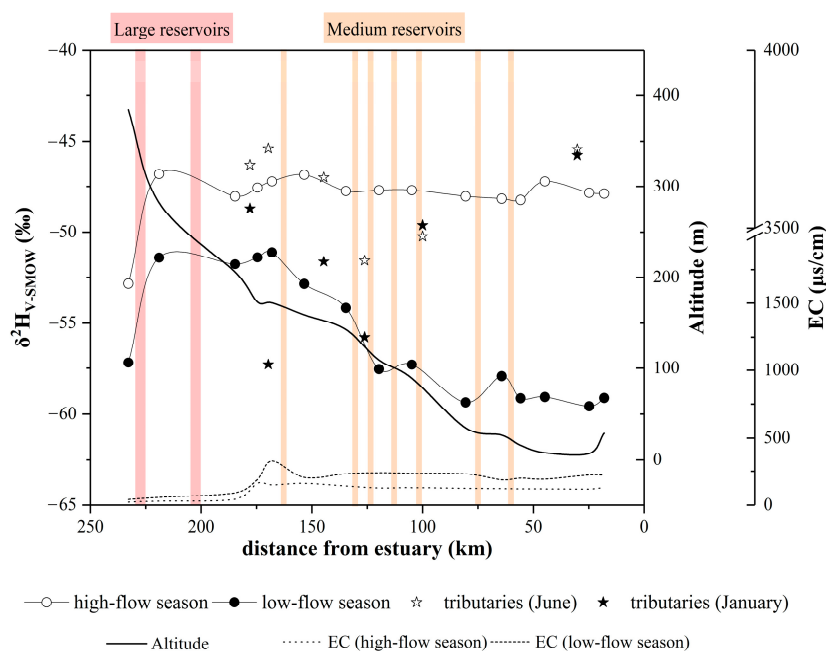


**Figure 7.** Hydrogen isotope composition and distribution of cascade reservoirs in the North River.

## 5. Conclusions

In the Jiulong basin, the river water's isotopic composition for high-flow and low-flow seasons showed different hydrological processes. The majority of river water samples had *d*-excess values indicating their main control by precipitation. The spatial characteristics of  $\delta^{18}\text{O}$  and  $\delta^2\text{H}$  were similar and originated from rainfall, despite also being influenced by geographic, temperature, and human activities, such as dams/reservoirs. The seasonal difference in river water isotopes, being heavier in summer and lighter in winter, suggested that the dominant precipitation isotope effect was rainfall amount and temperature in the study area. In addition, cascade reservoirs caused significant impacts on the Jiulong River. Thus, we demonstrated a complex hydrological process in the Jiulong River.

This study shows the spatial and seasonal characteristics of stable O and H isotopes in the Jiulong River, and we discussed the controlling factors for the variation. However, further research needs to be performed in the future, especially considering multiple water sources and modeling of river hydrological processes by O and H isotopes. The aim of this research is to demonstrate that measuring stable water isotopes is a good tracer of river water cycles driven by both natural environmental variability and anthropogenic activities.

**Author Contributions:** Conceptualization, K.Y. and G.H.; investigation, K.Y., G.H., M.L., X.L. and J.L.; methodology, K.Y. and Q.Z.; writing-original draft preparation, K.Y.; writing-review and editing, K.Y. and G.H.

**Funding:** This research was funded by the National Natural Science Foundation of China, grant number 41325010 and 41661144029.

**Acknowledgments:** We thank the anonymous reviewers for their valuable comments which greatly improve the manuscript. We also thank Yupeng Tian from China University of Geosciences, Beijing and Jing Ding and Changyi Lu from Institute of Urban Environment, Chinese Academy of Sciences for invaluable support in sampling.

**Conflicts of Interest:** The authors declare no conflict of interest.

## Appendix A

Table A1. Monthly rainfall in Xiamen during 2000–2018 [30].

Year	2000	2001	2002	2003	2004	2005	2006	2007	2008	2009	2010
January (mm month <sup>-1</sup> )	17.5	67.9	33.0	66.5	14.7	2.1	40.2	44.3	59.1	3.2	33.7
June (mm month <sup>-1</sup> )	524.1	324.0	79.6	190.9	67.5	186.3	169.5	378.3	361.7	203.3	252.2
Total annual rainfall (mm year <sup>-1</sup> )	1768.0	1512.9	1290.5	1091.4	1023.0	1350.0	1970.5	1219.8	1146.2	920.5	1470.9
January × 100/Total rainfall last year	/	3.8%	2.2%	5.2%	1.3%	0.2%	3.0%	2.2%	4.8%	0.3%	3.7%
June × 100/Total rainfall last year	/	18.3%	5.3%	14.8%	6.2%	18.2%	12.6%	19.2%	29.7%	17.7%	27.4%
Year	2011	2012	2013	2014	2015	2016	2017	2018	Average (2000–2018)		
January (mm month <sup>-1</sup> )	4.4	72.3	0.0	0.1	41.5	183.3	10.7	182.4	43.9		
June (mm month <sup>-1</sup> )	108.9	192.2	194.2	254.2	114.1	104.6	289.5	/	221.9		
Total annual rainfall (mm year <sup>-1</sup> )	916.7	1207.5	1663.1	1084.5	1480.9	2168.2	987.5	/	/		
January × 100/Total rainfall last year	0.3%	7.9%	0.0%	0.0%	3.8%	12.4%	0.5%	18.5%	/		
June × 100/Total rainfall last year	7.4%	21.0%	16.1%	15.3%	10.5%	7.1%	13.4%	/	/		

## References

- Henderson-Sellers, A.; McGuffie, K.; Noone, D.; Irannejad, P. Using stable water isotopes to evaluate basin-scale simulations of surface water budgets. *J. Hydrometeorol.* **2004**, *5*, 805–822. [\[CrossRef\]](#)
- Fekete, B.M.; Gibson, J.J.; Aggarwal, P.; Vorosmarty, C.J. Application of isotope tracers in continental scale hydrological modeling. *J. Hydrol.* **2006**, *330*, 444–456. [\[CrossRef\]](#)
- Meredith, K.T.; Hollins, S.E.; Hughes, C.E.; Cendon, D.I.; Hankin, S.; Stone, D.J.M. Temporal variation in stable isotopes (<sup>18</sup>O and <sup>2</sup>H) and major ion concentrations within the Darling River between Bourke and Wilcannia due to variable flows, saline groundwater influx and evaporation. *J. Hydrol.* **2009**, *378*, 313–324. [\[CrossRef\]](#)
- Good, S.P.; Noone, D.; Kurita, N.; Benetti, M.; Bowen, G.J. D/H isotope ratios in the global hydrologic cycle. *Geophys. Res. Lett.* **2015**, *42*, 5042–5050. [\[CrossRef\]](#)
- Reckerth, A.; Stichler, W.; Schmidt, A.; Stumpp, C. Long-term data set analysis of stable isotopic composition in German rivers. *J. Hydrol.* **2017**, *552*, 718–731. [\[CrossRef\]](#)
- Kendall, C.; Coplen, T.B. Distribution of oxygen-18 and deuterium in river waters across the United States. *Hydrol. Proc.* **2001**, *15*, 1363–1393. [\[CrossRef\]](#)
- Wang, Y.; Chen, Y.; Li, W. Temporal and spatial variation of water stable isotopes (<sup>18</sup>O and <sup>2</sup>H) in the Kaidu River basin, Northwestern China. *Hydrol. Proc.* **2014**, *28*, 653–661. [\[CrossRef\]](#)
- Han, G.; Lv, P.; Tang, Y.; Song, Z. Spatial and temporal variation of H and O isotopic compositions of the Xijiang River system, Southwest China. *Isot. Environ. Health Stud.* **2018**, *54*, 137–146. [\[CrossRef\]](#) [\[PubMed\]](#)
- Wu, H.; Zhang, X.; Li, X.; Li, G.; Huang, Y. Seasonal variations of deuterium and oxygen-18 isotopes and their response to moisture source for precipitation events in the subtropical monsoon region. *Hydrol. Proc.* **2015**, *29*, 90–102. [\[CrossRef\]](#)
- Lister, G.S.; Kelts, K.; Zao, C.K.; Yu, J.Q.; Niessen, F. Lake Qinghai, China: Closed-basin like levels and the oxygen isotope record for ostracoda since the latest Pleistocene. *Palaeogeogr. Palaeoclimatol. Palaeoecol.* **1991**, *84*, 141–162. [\[CrossRef\]](#)
- Jimenez-Madrid, A.; Castano, S.; Vadillo, I.; Martinez, C.; Carrasco, F.; Soler, A. Applications of hydro-chemical and isotopic tools to improve definitions of groundwater catchment zones in a karstic aquifer: A case study. *Water* **2017**, *9*, 595. [\[CrossRef\]](#)
- Martinelli, G.; Chahoud, A.; Dadomo, A.; Fava, A. Isotopic features of Emilia-Romagna region (North Italy) groundwaters: Environmental and climatological implications. *J. Hydrol.* **2014**, *519*, 1928–1938. [\[CrossRef\]](#)
- Bernal, S.; von Schiller, D.; Sabater, F.; Marti, E. Hydrological extremes modulate nutrient dynamics in mediterranean climate streams across different spatial scales. *Hydrobiologia* **2013**, *719*, 31–42. [\[CrossRef\]](#)

14. Spence, C.; Kokelj, S.V.; Kokelj, S.A.; McCluskie, M.; Hedstrom, N. Evidence of a change in water chemistry in Canada's subarctic associated with enhanced winter streamflow. *J. Geophys. Res. Biogeosci.* **2015**, *120*, 113–127. [[CrossRef](#)]
15. Liu, C.; Li, Z.; Dong, Y.; Chang, X.; Nie, X.; Liu, L.; Xiao, H.; Wang, D.; Peng, H. Response of sedimentary organic matter source to rainfall events using stable carbon and nitrogen isotopes in a typical loess hilly-gully catchment of China. *J. Hydrol.* **2017**, *552*, 376–386. [[CrossRef](#)]
16. Song, C.; Wang, G.; Liu, G.; Mao, T.; Sun, X.; Chen, X. Stable isotope variations of precipitation and streamflow reveal the young water fraction of a permafrost watershed. *Hydrol. Process.* **2017**, *31*, 935–947. [[CrossRef](#)]
17. Yan, D.; Liu, S.; Qin, T.; Weng, B.; Li, C.; Lu, Y.; Liu, J. Evaluation of TRMM precipitation and its application to distributed hydrological model in Naqu River Basin of the Tibetan Plateau. *Hydrol. Res.* **2017**, *48*, 822–839. [[CrossRef](#)]
18. Zafirah, N.; Nurin, N.A.; Samsurijan, M.S.; Zuknik, M.H.; Rafatullah, M.; Syakir, M.I. Sustainable ecosystem services framework for tropical catchment management: A review. *Sustainability* **2017**, *9*, 546. [[CrossRef](#)]
19. Brooks, J.R.; Wigington, P.J., Jr.; Phillips, D.L.; Comeleo, R.; Coulombe, R. Willamette River Basin surface water isoscape ( $\delta^{18}\text{O}$  and  $\delta^2\text{H}$ ): Temporal changes of source water within the river. *Ecosphere* **2012**, *3*, 1–21. [[CrossRef](#)]
20. Bowen, G.J.; Good, S.P. Incorporating water isoscapes in hydrological and water resource investigations. *Wiley Interdiscip. Rev. Water* **2015**, *2*, 107–119. [[CrossRef](#)]
21. Bowen, G.J.; Kennedy, C.D.; Liu, Z.; Stalker, J. Water balance model for mean annual hydrogen and oxygen isotope distributions in surface waters of the contiguous United States. *J. Geophys. Res. Biogeosci.* **2011**, *116*. [[CrossRef](#)]
22. Halder, J.; Terzer, S.; Wassenaar, L.I.; Araguas-Araguas, L.J.; Aggarwal, P.K. The Global Network of Isotopes in Rivers (GNIR): Integration of water isotopes in watershed observation and riverine research. *Hydrol. Earth Syst. Sci.* **2015**, *19*, 3419–3431. [[CrossRef](#)]
23. Penna, D.; Meerveld, H.J.V.; Zuecco, G.; Fontana, G.D.; Borga, M. Hydrological response of an Alpine catchment to rainfall and snowmelt events. *J. Hydrol.* **2016**, *537*, 382–397. [[CrossRef](#)]
24. Marchina, C.; Bianchini, G.; Natali, C.; Pennisi, M.; Colombani, N.; Tassinari, R.; Knoeller, K. The Po river water from the Alps to the Adriatic Sea (Italy): New insights from geochemical and isotopic ( $\delta^{18}\text{O}$ - $\delta\text{D}$ ) data. *Environ. Sci. Pollut. Res.* **2015**, *22*, 1–20. [[CrossRef](#)] [[PubMed](#)]
25. Natali, C.; Bianchini, G.; Marchina, C.; Knäller, K. Geochemistry of the Adige River water from the Eastern Alps to the Adriatic Sea (Italy): Evidences for distinct hydrological components and water-rock interactions. *Environ. Sci. Pollut. Res.* **2016**, *23*, 1–18. [[CrossRef](#)] [[PubMed](#)]
26. Rank, D.; Wyhlidal, S.; Schott, K.; Weigand, S.; Oblin, A. Temporal and spatial distribution of isotopes in river water in Central Europe: 50 years experience with the Austrian network of isotopes in rivers. *Isot. Environ. Health Stud.* **2018**, *54*, 115–136. [[CrossRef](#)] [[PubMed](#)]
27. Popescu, R.; Costinel, D.; Ionete, R.E.; Axente, D. Isotopic fingerprint of the middle Olt River basin, Romania. *Isot. Environ. Health Stud.* **2014**, *50*, 461–474. [[CrossRef](#)] [[PubMed](#)]
28. Guan, H.; Zhang, X.; Skrzypek, G.; Sun, Z.; Xu, X. Deuterium excess variations of rainfall events in a coastal area of South Australia and its relationship with synoptic weather systems and atmospheric moisture sources. *J. Geophys. Res. Atmos.* **2013**, *118*, 1123–1138. [[CrossRef](#)]
29. Gastmans, D.; Santos, V.; Galhardi, J.A.; Gromboni, J.F.; Batista, L.V.; Miotlinski, K.; Chang, H.K.; Govone, J.S. Controls over spatial and seasonal variations on isotopic composition of the precipitation along the central and eastern portion of Brazil. *Isot. Environ. Health Stud.* **2017**, *53*, 518–538. [[CrossRef](#)] [[PubMed](#)]
30. China Meteorological Data Service Centre Home Page. Available online: <http://data.cma.cn> (accessed on 31 July 2018).
31. Fujian Provincial Water Resources Department Home Page. Available online: <http://slt.fujian.gov.cn> (accessed on 31 July 2018).
32. Dansgaard, W. Stable isotopes in precipitation. *Tellus* **1964**, *16*, 436–468. [[CrossRef](#)]
33. Global Network of Isotopes in Precipitation Home Page. Available online: <https://nucleus.iaea.org/wiser> (accessed on 31 July 2018).
34. International Atomic Energy Agency. Available online: <https://www.iaea.org/wiser> (accessed on 31 July 2018).
35. Craig, H. Isotopic Variations in Meteoric Waters. *Science* **1961**, *133*, 1702–1703. [[CrossRef](#)] [[PubMed](#)]

36. Pang, Z.; Fan, Z.; Wang, J. The study on stable oxygen and hydrogen isotopes in the Zhangzhou Basin hydrothermal system. *Acta Petrol. Sin.* **1990**, *4*, 75–84.
37. Deng, K.; Yang, S.; Lian, E.; Li, C.; Yang, C.; Wei, H. Three Gorges Dam alters the Changjiang (Yangtze) river water cycle in the dry seasons: Evidence from H-O isotopes. *Sci. Total Environ.* **2016**, *562*, 89–97. [[CrossRef](#)] [[PubMed](#)]
38. Hu, C.; Froehlich, K.; Zhou, P.; Lou, Q.; Zeng, S.; Zhou, W. Seasonal variation of oxygen-18 in precipitation and surface water of the Poyang Lake Basin, China. *Isot. Environ. Health Stud.* **2013**, *49*, 188–196. [[CrossRef](#)] [[PubMed](#)]
39. Jiang, R.; Bao, Y.; Shui, Y.; Wang, Y.; Hu, M.; Cheng, Y.; Cai, A.; Du, P.; Ye, Z. Spatio-temporal variations of the stable H-O isotopes and characterization of mixing processes between the mainstream and tributary of the Three Gorges Reservoir. *Water* **2018**, *10*, 563. [[CrossRef](#)]
40. Ma, Q.; Zhang, M.; Wang, S.; Wang, B. Contributions of moisture from local evaporation to precipitations in Southeast China based on hydrogen and oxygen isotopes. *Prog. Geogr.* **2013**, *32*, 1712–1720.
41. Sun, C.; Li, X.; Chen, Y.; Li, W.; Stotler, R.L.; Zhang, Y. Spatial and temporal characteristics of stable isotopes in the Tarim River Basin. *Isot. Environ. Health Stud.* **2016**, *52*, 281–297. [[CrossRef](#)] [[PubMed](#)]
42. Chen, Y.; Du, W.; Chen, J.; Xu, L. Composition of hydrogen and oxygen isotopic of precipitation and source apportionment of water vapor in Xiamen Area. *Acta Scien. Circum.* **2016**, *36*, 667–674.
43. Hu, Y.; Liu, Z.; Zhao, M.; Zeng, Q.; Zeng, C.; Chen, B.; Chen, C.; He, H.; Cai, X.; Ou, Y.; et al. Using deuterium excess, precipitation and runoff data to determine evaporation and transpiration: A case study from the Shawan Test Site, Puding, Guizhou, China. *Geochim. Cosmochim. Acta* **2018**, *242*, 21–33. [[CrossRef](#)]
44. Cai, M.; Huang, Y.; Chen, M.; Liu, G. A study on hydrogen and oxygen isotopes composition of precipitation in Xiamen. *J. Oceanogr. Taiwan Stra.* **2000**, *19*, 446–453.
45. Chen, J.; Cao, J.; Huang, Y. The hydrogen and oxygen isotope composition of precipitation in the Xiamen coastal area. *J. Mar. Sci.* **2010**, *28*, 11–17.
46. Liu, H.; Guo, Z.; Gao, A.; Yuan, X.; Zhang, B.  $^{18}\text{O}$  and  $^{226}\text{Ra}$  in the Minjiang River estuary, China and their hydrological implications. *Estuar. Coast. Shelf Sci.* **2016**, *173*, 93–101. [[CrossRef](#)]
47. Wang, C.; Lian, E.; Yang, C.; Deng, K.; Li, C.; Yang, S.; Yin, P. Stable isotopes of Hydrogen and Oxygen in small rivers of Zhejiang and Fujian Provinces and their temporal and spatial variations. *Mar. Geol. Quat. Geol.* **2018**, *38*, 160–169.
48. Wei, K.; Lin, R. The influence of the monsoon climate on the isotopic composition of precipitation in China. *Geochimica* **1994**, *23*, 32–41.
49. Ogrinc, N.; Kanduc, T.; Stichler, W.; Vreca, P. Spatial and seasonal variations in  $\delta^{18}\text{O}$  and  $\delta\text{D}$  values in the River Sava in Slovenia. *J. Hydrol.* **2008**, *359*, 303–312. [[CrossRef](#)]
50. Zhang, Z.; Huang, Y.; Huang, J. Hydrologic alteration associated with dam construction in a medium-sized coastal watershed of Southeast China. *Water* **2016**, *8*, 317. [[CrossRef](#)]

